

# COOLING FRONT MEASUREMENT OF A 9-CELL CAVITY VIA THE MULTI-CELL TEMPERATURE-MAPPING SYSTEM AT CORNELL UNIVERSITY

M. Ge<sup>#</sup>, R. Eichhorn, F. Furuta,  
Cornell University, Ithaca, NY 14853, USA

## Abstract

Cooling speed significantly affects flux trapping of a SRF cavity, which will determine the residual resistance and the quality factor of the cavity. We measured the temperature distribution of a 9-cell cavity at different cooling speeds by the multi-cell T-map system of Cornell University. This paper proposed a method to evaluate the formation of a normal conducting island at different cooling speed. The fast cool-down and slow cool-down has been compared. We conclude that the slow cool-down freezes less normal conducting islands.

## INTRODUCTION

For the future accelerators, the high quality factor of SRF cavities will reduce the cryogenic cost and operation cost. Hence the surface resistance should be kept as low as possible. Recent tests of cavities suggested that the cooling speed impacts the quality factor significantly when the cavity transits from normal conducting state to superconducting. The first observation was reported by HZB in 2011[1]. They stated that the slow cool-down can do the better external magnetic field expulsion. Cornell University observed quite similar results from ELR 7-cell horizontal test by several thermal cycles [2]. The Q-value had been increased by factor 2 due to the slow cool-down. However, the nitrogen-doped cavities can achieve high-Q benefited from the fast cool-down [3-4], which is contradict to the observation in [1-2]. The discussion was focus on how the cooling speed affects the cooling uniformity of a cavity. As Cornell's multi-cell temperature-mapping system has unique capabilities, we started investigating cool-down dynamics of multi-cell cavities to get an understanding how the transition region between the normal and the superconducting state moves along the cavity.

## THE EXPERIMENT SET-UP

The Cornell multi-cell Temperature-map system [5, 6] has nearly two thousand thermometers. The temperature sensor is a 100Ω carbon Allen-Bradley resistor (5% 1/8 W). The sensors are pushed tightly to against cavity exterior surface by Pogosticks and springs. APIEZON type N grease, which has good thermal conductivity at low temperature, is applied to fill the gap between the sensors and the surface. The T-map system is consisted of two sets of 3-cell boards and one set of 1-cell boards. One set has 24 boards attached azimuthally in every 15 degree

on a cavity. Thus the system is capable to measure up to seven cells of a multi-cell SRF cavity. In this experiment, we mounted the T-map on the middle seven cells of a TESLA-shape 9-cell cavity which is shown in Fig. 1. The 9-cell cavity in Fig. 1 has been vertically mounted on an insert. The main coupler port is on bottom side; the board number 1 in every set has same angle with the main coupler port. In this paper, we only consider the T-map covered cells and define the cell numbers 1 to 7 from top to bottom. The T-map system has 5 channels to connect electronics (depicted in Fig. 1 (Right)); the channel 1 and 2 scan the top three cells, the channel 3 scans the middle cell, and the channel 4 and 5 scan the bottom three cells. The T-map electronic scans 5 channels simultaneously; it takes one minute for the electronics to scan all the T-map sensors. A Matlab program records the resistance value of each T-map sensor. The T-map was continuously running during the cavity cool down and warm up, therefore the T-map can capture the temperature variation versus time.

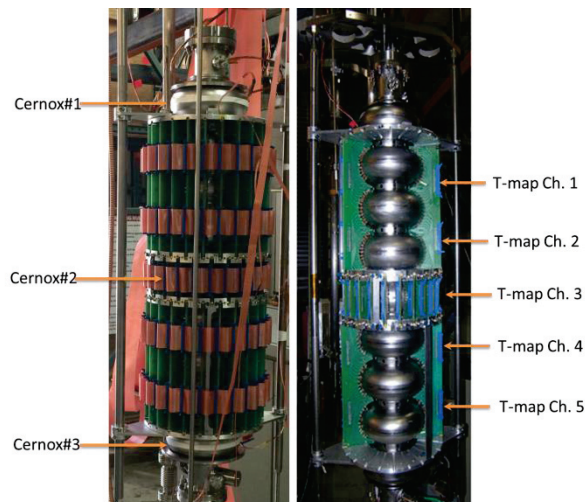


Figure 1: (Left) The multi-cell temperature-mapping system mounted on a TESLA-shape 9-cell SRF cavity, (Right): Several T-map boards have been removed to expose the cavity.

## Calibration

As the T-map can only record the resistance value of each sensor, it needs to convert it into temperature value. In a calibration, we change ambient temperature surrounding the T-map sensors recording the resistance of each T-map sensor and the ambient temperature simultaneously. Hence the relation between the resistance and the temperature is possible to be established. The key

<sup>#</sup>mg574@cornell.edu

point of the calibration is how uniform the ambient temperature is changed. The ideal case is the thermal gradient between sensors to sensors should be close to zero during the temperature changing. In this experiment, we utilized three Cernox sensors which were mounted on the top, middle and bottom of the cavity to monitor the ambient temperatures. The set-up is shown in Fig. 1 (Left). The calibration data was taken during the cavity slowly warm-up from 4.2K to 50. Figure 2 shows the temperatures taken by the Cernox vs. time during the warm-up. The whole process took about 3 hours. The temperature gradients between the cavity top and bottom are small enough to be neglected. Thus we can use a single temperature value to represent the ambient temperature at a moment in the calibration.

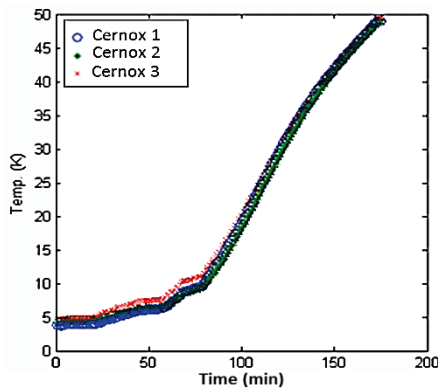


Figure 2: Temperature vs. time during cavity warm-up.

A calibration curve of a T-map sensor is shown in Fig. 3. The resistance value varies from 300Ω to 1600Ω when the temperatures changed from 50K to 4.2K. The curves can be fitted by a third order polynomial function shown in equation (1). The coefficients of the polynomial function can be obtained after the fitting for every T-map sensors.

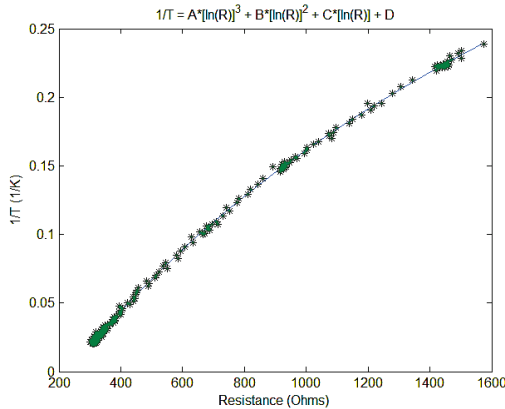


Figure 3: A calibration curve of a temperature sensor.

$$\frac{1}{T} = ax^3 + bx^2 + cx + d, \quad (1)$$

$$x = \ln(R).$$

Here  $T$  is the temperature;  $R$  is the resistance of the T-map resistor;  $a$ ,  $b$ ,  $c$ , and  $d$  are the fitting coefficients of a sensor.

The T-map results then can be converted from the resistance values into the temperature values by the calibration curves. A converted result of the T-map is displayed in a 2D colour-map (Fig. 4). The T-map results are essentially a 2D array with 77 rows and 24 columns. Each  $11 \times 24$  sub-array represents one cell; the temperature value is depicted by colours. The channel 2 broke during the experiment; hence we don't have data of the cell 3 and bottom half of the cell 2. But this flaw doesn't affect conclusions of the experiment.

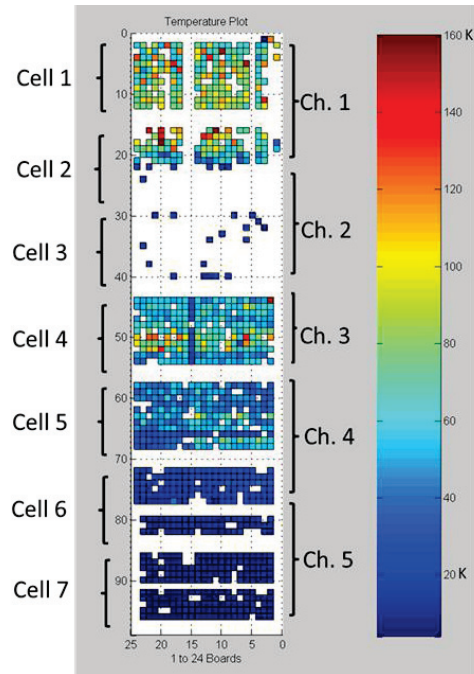


Figure 4: A T-map result in temperature displayed in a 2D colour-map.

### Slow and Fast Cool Down

For the slow cool down, we used a short liquid-helium transfer line the end of which was above the 9-cell cavity. During the transfer, the liquid helium uniformly sprayed on the cavity like a shower. The whole cooling was taken about 6 hours from room temperature to 4.2K. We continuously took data from the T-map as well as the Cernox. The detail positions of the three Cernox sensors are shown in Fig. 1. Figure 5 is the temperature versus time curves measured by the Cernox sensors. The Cernox 1 indicates the temperature on the top of the cavity; while the Cernox 2 indicates the temperature on the bottom. Thus the measurement suggests the thermal gradient from the cavity top and the bottom is fairly small in the whole slow cool down.

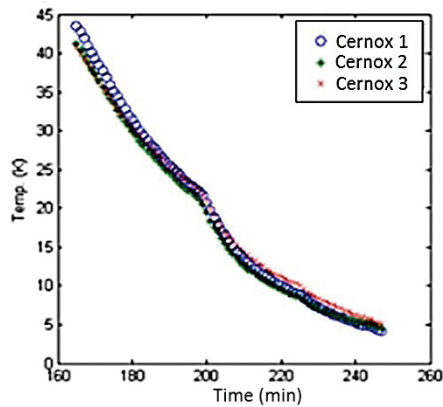


Figure 5: The temperatures versus time curves measured by the Cernox sensors in the slow cool down.

As people are more interested in the temperature distribution when the cavity was passing the critical temperature (9.27K for Nb). We exhibit the T-map results in Fig. 6. The T-map results are consistent with the Cernox measurement, but with more details. From the colour-bar we know that the most temperature value concentrates in 8K-10K regions. Few red points which located in cell 3 and bottom cell 2 regions are due to the bad connection of the channel 2; it's not real.

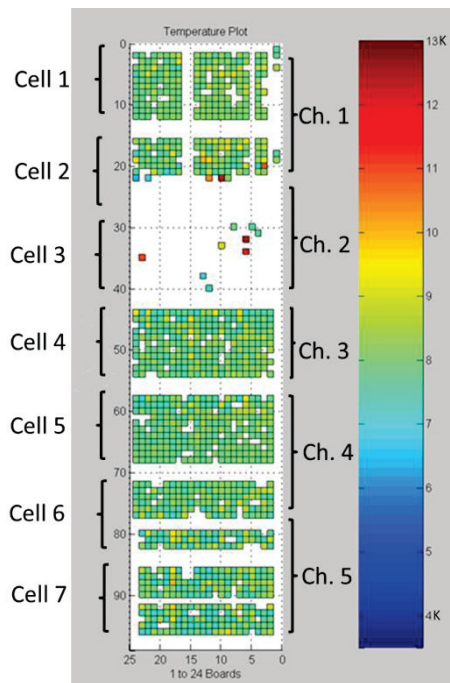


Figure 6: The T-map results when the cavity was passing the 9.27K in the slow cool down.

While in the fast cool down, we used a long transfer line which extends its end to the bottom of our Dewar, thus it can cool the 9-cell cavity from its bottom cell. The whole process took less than an hour. Figure 7 displays the thermal gradient between the cavity top and the bottom. When the bottom Cernox sensor passed 9.27K, the thermal gradient between the top and the bottom is

approximately 160K-200K, which is much larger than the slow cool down.

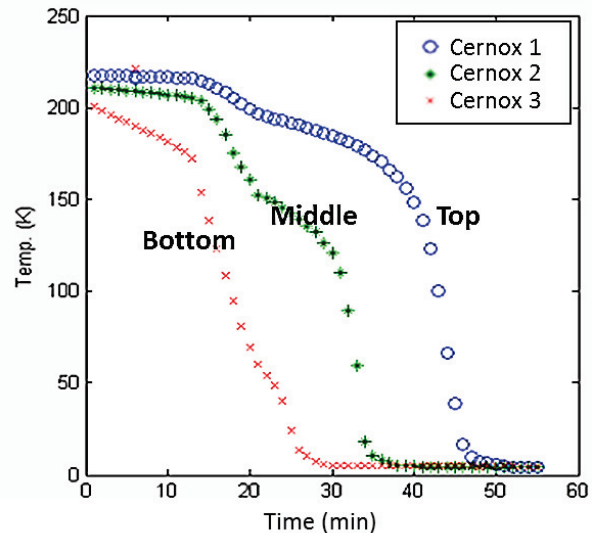


Figure 7: The temperatures versus time curves measured by the Cernox sensors in the fast cool down.

Differed with the slow cool down, the cavity did not pass the 9.27K at same time. The cells from the bottom were cooled one by one. The T-map results revealed the cooling front moving from the cavity bottom to the top, which is depicted in Fig. 8. Here we set the colour-bar from 4.2K to 160K to exhibit the thermal gradients clearly. Figure 8 (1) shows the moment when the cell 7 started to be cooled; the temperatures on the cell 7 were around 40K-60K. Fig. 8 (2) shows the moment when it is 2 minutes later than Fig. 8 (1). The cooling front was moving up from the cell 7 to cell 6. The Temperature on the bottom region of the cell 7 was close to 4.2K. Figure 8 (3) is 4 minutes after Fig. 8 (1), which exhibited the cooling front was moving up further.

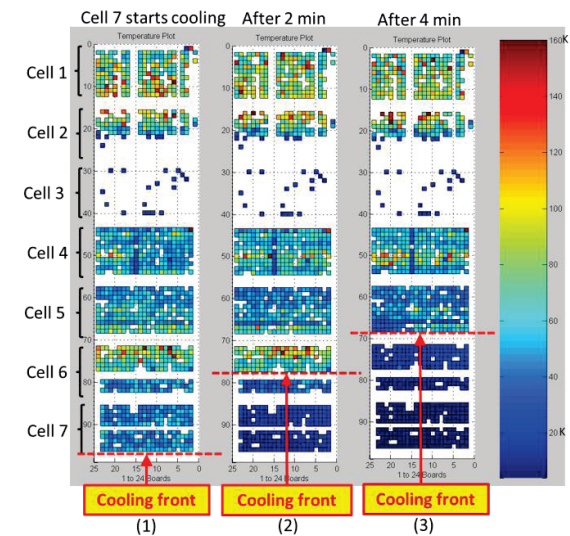


Figure 8: The T-map results showed the cooling front movement in the fast cool down.

Our analysis will try to quantify the spatial uniformity of the transition of the superconductivity.

### THE DATA ANALYSIS

The most interesting thing is to identify the thermal gradient magnitude when the cavity passes the 9.27K, because smaller thermal gradient has less chance to freeze the normal conducting islands on cavity surface, hence it has less chance to freeze the flux on cavities. The purpose of this analysis is to demonstrate that the slow cool down has much less thermal gradient than the fast cool down. Hence the slow cool down freezes less flux than the fast cool down.

As the T-map result is a 77×24 array, we set a selection window of temperature between 9-9.5K, to calculate the average temperature difference by equation (2).

$$\Delta T = \frac{1}{N} \sum_{i=1}^{77,24} \frac{1}{4} (|T_{ij} - T_{i\pm 1,j}| + |T_{ij} - T_{i,j\pm 1}|). \quad (2)$$

Here  $N$  is the number of the selected elements in the window. In equation (2), it calculates the average temperature differences between the element and its four adjacent elements in one T-map scan. The number  $N$  in the slow cool down is much larger than in the fast cool down due to their character we described in the previous section. Therefore this number  $N$  normalized the fast cool and the slow cool, which allows us to compare them. In Fig. 9, we plot the average  $\Delta T$  versus time of the slow cool and the fast cool. It shows the average temperature of the fast cool is larger than the slow cool, when the portion of the cavity becomes superconducting.

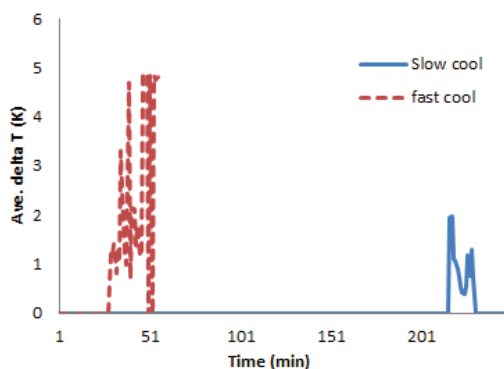


Figure. 9: The average  $\Delta T$  versus time curves of the slow cool and the fast cool.

We also plot average  $\Delta T$  versus surface temperature in Fig. 10. We have two sets of data to compare the fast and slow cool-down. It clearly shows that the thermal gradient of the slow cool is around 0.5K-2K, which is much less than 5K-8K in the fast cool down.

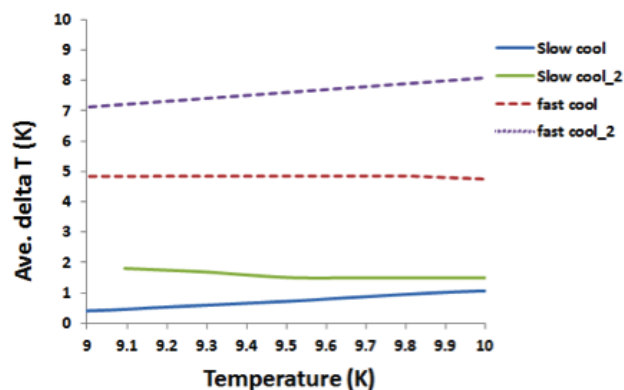


Figure 10: The average  $\Delta T$  versus temperature comparison between the slow cool and the fast cool in fine temperature scale.

### CONCLUSION

We described how a T-map could help understanding the cool-down dynamics for different cycles. We found visualizations in the form of Figure 3 and 4 to be sometimes misleading in judging about the homogeneity of the cool-down. As a consequence, we developed a metric, given in (2) which allows quantifying the temperature variances of the cavity as regions become superconducting. From that we conclude that a fast cool-down has larger temperature gradients at transition.

However, we see this as a first approach to quantify the cool-down uniformity. It also remains open, if smaller temperature gradients result in a smaller probability of creating normal conducting islands or vice versa, which is a topic of our on-going studies.

### REFERENCES

- [1] O. Kugeler, *et al.*, “Improving the Intrinsic Quality Factor of SRF Cavities by Thermal Cycling”, Proceedings of SRF2011, Chicago, IL USA (2011) 724.
- [2] N. Valles, *et al.*, “Cornell ERL Main Linac 7-Cell Cavity Performance in Horizontal Test Cryomodule Qualification”, Proc. of the 2013 Int. Conf. on Part Acc., Shanghai, China (2013) 2459.
- [3] A. Romanenko, *et al.*, “Dependence of the residual surface resistance of SRF cavities on the cooling rate through  $T_c$ ”, arXiv:1401.7747.
- [4] A. Romanenko, *et al.*, Sergatskov, “Dependence of the residual surface resistance of superconducting RF cavities on the cooling dynamics around  $T_c$ ”, arXiv:1401.7747
- [5] M. Ge, *et al.*, “Construction, Evaluation, and Application of a Temperature Map for Multi-cell SRF Cavities”, IPAC12.
- [6] M. Ge, *et al.*, “A temperature-mapping system for multi-cell SRF accelerating cavities”, Proc. Of PAC2013, CA USA.